Understanding Sentinel-1 backscatter response to sugarcane yield variability and waterlogging

den Besten, Nadja; Steele Dunne, Susan; Mahmud, Ashfak; Jackson, Daniel; Aouizerats, Benjamin; de Jeu, Richard; Burger, Rogier; Houborg, Rasmus; McGlinchey, Mark; van der Zaag, Pieter

DOI
10.1016/j.rse.2023.113555

Publication date
2023

Document Version
Final published version

Published in
Remote Sensing of Environment

Citation (APA)
den Besten, N., Steele Dunne, S., Mahmud, A., Jackson, D., Aouizerats, B., de Jeu, R., Burger, R., Houborg, R., McGlinchey, M., & van der Zaag, P. (2023). Understanding Sentinel-1 backscatter response to sugarcane yield variability and waterlogging. *Remote Sensing of Environment*, *290*, Article 113555. https://doi.org/10.1016/j.rse.2023.113555

Remote Sensing of Environment 290 (2023) 113555

Contents lists available at ScienceDirect

Remote Sensing of Environment

journal homepage: www.elsevier.com/locate/rse

Understanding Sentinel-1 backscatter response to sugarcane yield variability and waterlogging

Nadja den Besten [a,d,*], Susan Steele Dunne [b], Ashfak Mahmud [e], Daniel Jackson [a], Benjamin Aouizerats [a], Richard de Jeu [a], Rogier Burger [a], Rasmus Houborg [a], Mark McGlinchey [f], Pieter van der Zaag [c,d]

[a] Planet Labs Inc, San Francisco, CA 94107, USA
[b] TU Delft, Department of Geoscience and Remote Sensing, Delft, The Netherlands
[c] IHE Delft Institute for Water Education, Delft, The Netherlands
[d] TU Delft, Department of Water Management, Delft, The Netherlands
[e] University of Helsinki, Department of Geosciences and Geography, Helsinki, Finland
[f] SQR Software, Pietermaritzburg, 3201, South Africa

ARTICLE INFO

Edited by Marie Weiss

Keywords:
Sentinel-1
Agriculture
Waterlogging
Synthetic Aperture Radar (SAR)
Crop monitoring
Sucrose
Sugarcane yield

ABSTRACT

Sentinel-1 observes the whole globe every 12 days (6 days when both satellites were operational) and provides a wealth of data relevant to agriculture. Sugarcane cultivators could potentially benefit from these data by using them to assist operational and management practices. However, first, thorough understanding is needed of Sentinel-1 backscatter and its behavior over sugarcane canopies. In this study, we aimed to improve understanding of how Sentinel-1 backscatter responds to sugarcane yield variability and waterlogging. In order to do so we focused on an irrigated sugarcane plantation in Xinavane, Mozambique. In the analysis presented, we assessed different polarizations, their ratio, and benchmarked them against optical indices and passive microwave observations in different seasons. With the help of a large sugarcane yield dataset, we analyzed how backscatter relates to sucrose yield variability in different seasons. We found VV backscatter related to the stalk development, the most important reservoir for sucrose accumulation. In addition, in a season with reported waterlogging, optical and radar observations showed a delay in sugarcane crop development. Further analysis showed the presence of water underneath the canopy caused an increase in all polarizations and the cross ratio (CR). The results imply that Sentinel-1 backscatter contains information on both waterlogging under the canopy as well as sucrose development in the stalk. By isolating and quantifying the impact of waterlogging on backscatter, it will be possible to further quantify sucrose development with backscatter observations and identify waterlogging simultaneously.

1. Introduction

The global production of sugarcane is driven by the demand for raw sugar and (bio-)ethanol (Shabbir et al., 2021). Over the last few decades researchers have managed to breed the perennial grass to produce high contents of sucrose. Furthermore, sucrose is the soluble sugar present in the stem of the sugarcane crop and, as a result of breeding, sugarcane species accumulate high concentrations of sucrose. Additionally, the concentration of sucrose in the sugarcane stem can be as high as 18 percent of fresh weight (Mustafa et al., 2018).

Improving operational and management practices in the sugarcane production chain are key to sustainable intensification, in order to ultimately close the current yield gaps with less pressure on the environment (Bordonal et al., 2018). An example is to improve current manual sugarcane monitoring to adjust on-site management (Bocca et al., 2015). Here, information on the presence of waterlogging plays a role due to waterlogged soil conditions affecting plant physiology and hampering crop growth and yield significantly (Shaw et al., 2013; den Besten et al., 2021b). Academic literature reports the cause of waterlogging in irrigated agriculture to be a result of over-irrigation or poor sub-surface drainage (FAO, 2016). In rain-fed agriculture, Martinez-Feria and Basso (2020) found waterlogging to be an important driver behind yield instability in the US Midwest.

Satellite remote sensing can play a role in improving current sugarcane production practices through monitoring (Cancela et al., 2019; McCabe et al., 2016; Mancini et al., 2019; Bégué et al., 2018). Unfortunately, the integration of new remote sensing techniques into the

* Corresponding author at: Planet Labs Inc, San Francisco, CA 94107, USA.
E-mail address: nadja@planet.com (N. den Besten).

https://doi.org/10.1016/j.rse.2023.113555
Received 18 November 2022; Received in revised form 15 March 2023; Accepted 20 March 2023
Available online 27 March 2023

decision making process of sugarcane production remains slow (Bocca et al., 2015). Previous studies have researched the relationship between sugarcane yield and vegetation indices computed from satellite data (Bégué et al., 2010; Lofton et al., 2012; Molijn et al., 2019; Morel et al., 2014). Common techniques are based on optical indices (e.g. NDVI) (Morel et al., 2014) and focus on machine learning (Shendryk et al., 2021; Fernandes et al., 2017).

Vegetation indices retrieved from backscatter are also starting to proliferate (Steele-Dunne et al., 2017). Researchers have shown the capabilities of cross- and co-polarization backscatter channels to monitor sugarcane (Baghdadi et al., 2009; Molijn et al., 2019; Som-ard et al., 2021). For example, Baghdadi et al. (2009) concluded cross-polarizations are slightly better for monitoring sugarcane and, therefore, Molijn et al. (2019) did not consider co-polarization.

Vegetation indices retrieved from radar are sensitive to different characteristics than indices derived from optical sensors. Microwave energy responds to the dielectric properties of the crop canopy, but also to the structure of the crops, such as the size, and orientation of leaves, stalk, and fruit (McNairn and Brisco, 2004). The dielectric properties are strongly influenced by the water content in the plant (Ulaby and Jedlicka, 1984). In addition, for sugarcane, den Besten et al. (2021a) showed how a change in the internal characteristics of sugarcane during the growing season influences the radar backscatter. As a result of sucrose accumulation, the dielectric constant of the canopy decreases and the strength of the observed backscatter signal also decreases.

Unfortunately, studies relating large sugarcane yield datasets to backscatter are scarce (den Besten et al., 2021a; Shendryk et al., 2021). In addition, it is not known how or the extent to which waterlogging beneath a thick canopy, such as sugarcane, affects different radar polarizations and polarization ratios. Expanding knowledge on how Sentinel-1 backscatter responds to sugarcane yield variability and waterlogging is crucial to help the interpretation of the radar vegetation signals. In addition, information on the presence of waterlogging itself is valuable to several agricultural practices (e.g. drainage issues, trafficability, irrigation).

Therefore, the aim of this study was to understand how Sentinel-1 backscatter responds to sugarcane yield variability and waterlogging. Here we present how backscatter observations can be used to monitor sugarcane yield and how the observations are influenced by waterlogging. The ultimate goal was to increase understanding on how to simultaneously monitor sugarcane and waterlogging using Sentinel-1 SAR data. To research the issue we focused on an irrigated sugarcane plantation in Xinavane, southern Mozambique, a site with numerous reported issues related to waterlogging (den Besten et al., 2021b).

2. Sugarcane growth

Sugarcane is grown in subtropical and tropical regions. Harvest dates are ideally determined to match optimum supply to the nearest sugar mill (Bocca et al., 2015). The majority of sugarcane plantations or farms grow sugarcane as a ratoon crop (Inman-Bamber, 2013). This is a common and cost-effective practice around the world, where sugarcane is not replanted after harvest, but grown from the preceding plant (Surendran et al., 2016).

Sugarcane is ideally harvested at maximum sugar accumulation in the stem. The average length of the growing season in Xinavane is twelve months (den Besten et al., 2020). The growing season can be divided into different growth stages. In the analysis presented in this paper, we defined the following four growth stages: the initial stage (30 days), the tillering stage (90 days), the development stage (150 days), and the final stage (90 days) (Doorenbos and Kassam, 1979; Silva et al., 2015).

Sugarcane is a peculiar crop as it accumulates sucrose both inside and outside the cells (both symplast and apoplast) (Wang et al., 2013). The sugarcane plant deposits the sucrose in the stem vacuoles and cells around it. During the tillering stage, the sugarcane plant starts accumulating biomass. The biomass growth takes place particularly in the leaf canopy (Inman-Bamber, 2013). Hereafter, in the development stage, the growth emphasis is on the stem, which is an important sink for sucrose development (Inman-Bamber, 2013; Cock, 2001). In this stage, the sucrose accumulation starts to play a significant role. See Fig. 1 (A) and (D). Sucrose forms as a hydrogen bond, and the development of stalk moisture and sucrose are therefore closely linked to each other (Inman-Bamber et al., 2009). Over time, the sucrose accumulation ensures that a fraction of the water in the fresh stalk is substituted with sucrose, see Fig. 1 (A) (Muchow et al., 1996).

Throughout the growing season, the vertical distribution of sucrose and Vegetation Water Content (VWC) inside the sugarcane plant changes as well. From our experience in Xinavane, we know that the vertical distribution inside the sugarcane plant changes during the growing season. However, to our knowledge, quantitative data on this have not been published to date. A few researchers have attempted to capture the changes of the vertical distribution over time by sampling different varieties in the development stage. These results showed the sucrose distribution in lower yielding varieties was stored mostly in the lower inter-nodes, whereas in the higher yielding varieties the sucrose is distributed more homogeneous in the stalk, see Fig. 1 (C) and (D) (Inman-Bamber et al., 2009). Nodes are referred to as the place where leafs develop on the stalk, see Fig. 1 (E) and (F).

3. Data and methods

The research presented in this paper focused on different satellite remote sensing observations for an irrigated sugarcane plantation. Optical and passive microwave observations were used to benchmark Sentinel-1 observations, in order to understand the seasonal characteristics and expose differences. Ground data were used to understand how radar observations in different polarizations and their ratio relate to sucrose yield. Section 3.1 will explain the origin and characteristics of the data and Section 3.2 will provide a description of the data analysis.

3.1. Data

3.1.1. Yield data

Crop yield data were obtained from a sugarcane plantation located on the banks of the lower Incomati river in Xinavane, Mozambique (see Fig. 2). The local sugar mill runs from April to December and during these months sugarcane is harvested and milled. The sugarcane produced in the plantation is converted to raw sugar at the sugar mill. In the plantation, ratoon sugarcane is grown under irrigated conditions (den Besten et al., 2020). The average field-size is approximately 20 hectares (den Besten et al., 2020). The sugarcane in the plantation is planted in rows 1–1.5 meter apart. The dominant sugarcane varieties in the plantation are N25 and N23, accounting for 86 percent (Butler, 2001). The research presented focused on 299 fields that are owned and managed by the Tongaat Hulett group.

To harvest the sugarcane, fields are burnt to ease the manual harvest process and remove leaves. After the fire ceases, the harvest laborers cut the stalk from the roots at ground level. The harvested sugarcane is then collected by trucks allocated to specific fields. The trucks containing harvested sugarcane are weighed and documented per field. After weighing, several samples are tested for their sucrose content. This process results in data per field on sugarcane yield (tonnes of cane per hectare, TCH) and sucrose yield (tons of sucrose per hectare, TSH).

For this research we considered the sucrose yield (TSH) obtained by the sugar mill for the seasons 2018–2019, 2019–2020, and 2020–2021. The preceding seasons correspond to 2019, 2020, and 2021 in Fig. 3 (A). These years were taken because of robust availability of satellite data during these seasons and contrasting years in terms of soil water content. Seasons 2015–2019 experienced a rainy season below average, in contrast to seasons 2020 and 2021 in Fig. 3 (den Besten et al., 2020).

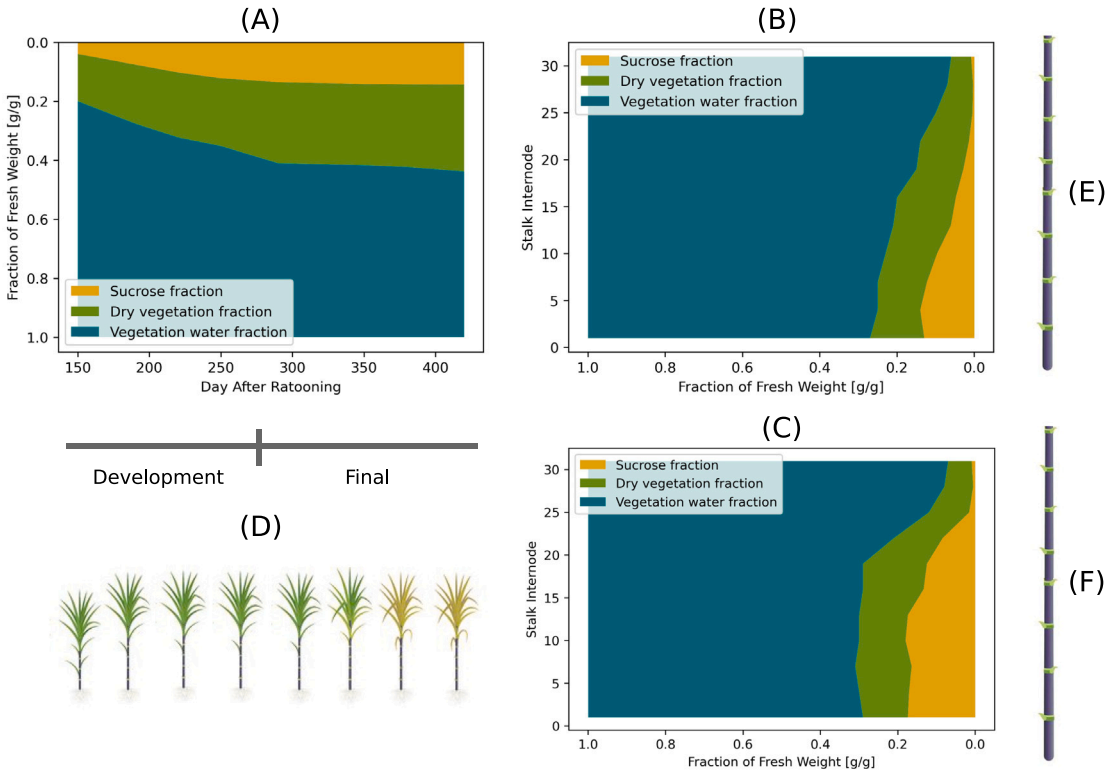

Fig. 1. A schematic diagram of the vertical and temporal distribution of sucrose in the sugarcane stalk. (A) shows the temporal change of sucrose, vegetation, and water distribution over the development and final phase (Muchow et al., 1996); (B) and (C) the vertical distribution for a low and high yielding variety respectively (Inman-Bamber et al., 2009) For reference purposes (D), (E), and (F) illustrate the physical development of the canopy and vertical structure of the sugarcane stalks.

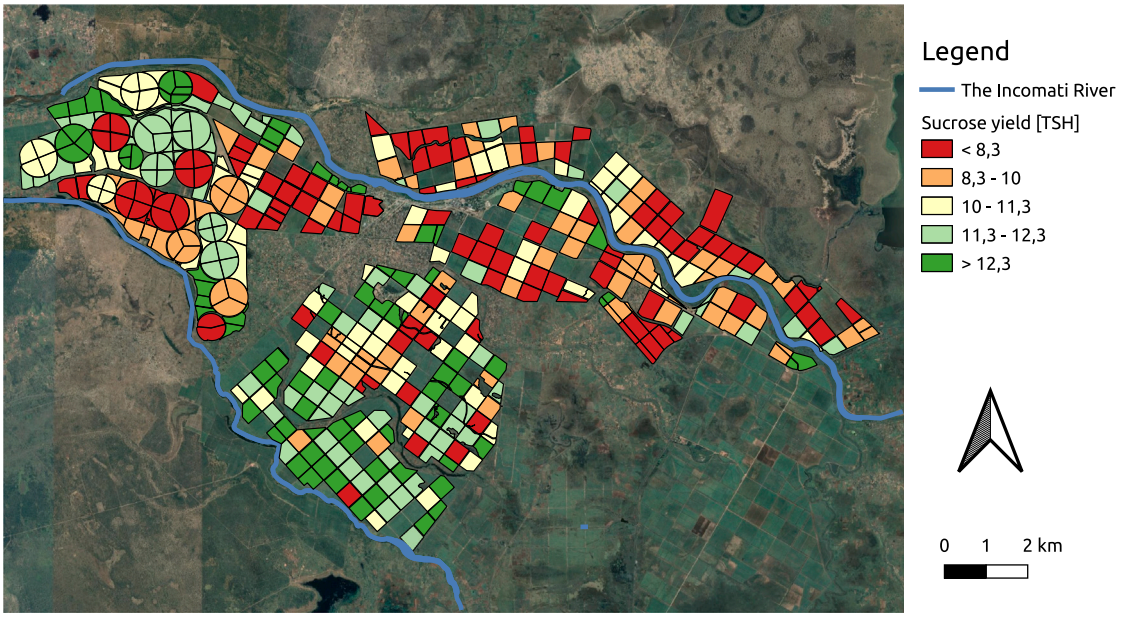

Fig. 2. Location of fields under study in Xinavane, Mozambique. The colors indicate average yield for the seasons 2019–2021 for 299 fields. (For interpretation of the references to color in this figure legend, the reader is referred to the web version of this article.)

Interestingly, Fig. 3 (A) shows the mean sucrose yield was lower in seasons 2020 and 2021.

In addition, Fig. 3 (B) shows the percentage of sucrose and moisture of fresh weight measured at harvest. This is to illustrate the high percentage of sucrose concentration in the stalk (up to 16 percent). There is a negative correlation between sucrose and moisture content at harvest, further illustrating the relation between sucrose and moisture content in the sugarcane stalk (see Section 2).

3.1.2. Soil Water Content and Land Surface Temperature

During the analysis, Soil Water Content and Land Surface Temperature as derived from the Land Parameter Retrieval Model using

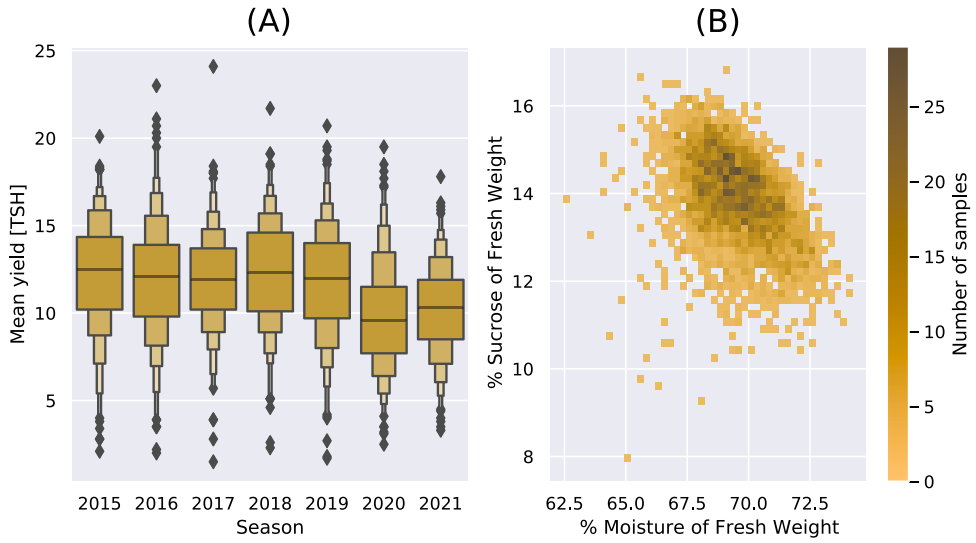

Fig. 3. (A) shows a boxplot of mean sucrose yield for seasons 2015 until 2021 (B) shows the relation between measured sucrose and moisture percentage of fresh weight of seasons 2018–2021 for the 299 fields.

passive microwave observations were used (van der Schalie et al., 2017; Owe et al., 2008). A downscaling method was applied to the passive microwave brightness temperatures to get to a spatial resolution of 100 m (de Jeu et al., 2016). The basis for Soil Water Content was SMAP's L-band (1.41 GHz) passive microwave observations at 06:00AM at equatorial passing (descending) and the effective field of view footprint is a 39 km by 47 km ellipse. The observations represent the Soil Water Content in the first 0–5 cm of the soil. To compute Land Surface Temperature AMSR-2's Ka-band (36.5 GHz) data were used, which observes at 01:30AM (descending) with a spatial resolution of 7 km × 12 km (Holmes et al., 2009; Owe et al., 2008).

For the analysis, the Soil Water Content was used to understand the temporal variation in soil moisture over the three seasons. The data products are too coarse to identify individual irrigation events (den Besten et al., 2021b). Nevertheless, it is very valuable for identifying wet or dry periods. Certainly, in combination with observations from the field, a period with prolonged waterlogging could be identified in season 2020–2021, see Fig. 4 and Section 3.2.4. In Fig. 4 (C) we zoom in on the soil water content during the identified waterlogging peak where (II) indicates a week during the waterlogging peak and (I) a week before of the waterlogging event.

Fig. 4 (A) also shows the average daily Land Surface Temperature for all the fields under study. The LST reflects the seasonality in the plantation, with higher temperatures before and during the rainy season and lower temperatures during winter. LST was used in the analysis to understand seasonal dynamics and to understand the role of temperature on sucrose development.

3.1.3. Sentinel-1 radar backscatter

Sentinel-1 GRD data were processed using Google Earth Engine and the Sentinel-1 Toolbox. During this process, a radiometric calibration and terrain correction were applied to convert the data into normalized backscatter and correct for elevation differences. The Sentinel-1 satellites observed with Synthetic Aperture Radar (SAR), captures backscatter at 5.405 GHz (C-band) at 5x20 m spatial resolution. Descending data from Sentinel-1 A and B were used. Fig. 5 (A) shows the available observations that were used throughout the season. In southern Mozambique the majority of the revisit frequency between 4 to 6 days, with a few exceptions in 2018 as a result of maintenance (ESA, 2021). Fig. 5 (B) provides a snapshot of Sentinel-1 VH polarization. Finally, the observations were sampled at a 10 by 10 meter resolution.

Backscatter time series were extracted for each field with daily average values of VV and VH polarizations, see Fig. 2 (B) for the respective field boundaries. The cross ratio (CR) was also calculated for each field. The Cross Ratio can be calculated by subtracting VH-VV on a logarithmic scale. Previous work showed CR reduces the backscatter effect of soil moisture and soil-vegetation interactions (Vreugdenhil et al., 2018; Khabbazan et al., 2019). The individual VV and VH backscatters contain artefacts of soil moisture, rain events, and irrigation for example (Molijn et al., 2019). The CR relates more to the volume scattering from vegetation and increases with vegetation growth (Veloso et al., 2017).

3.1.4. Planet Fusion NDVI

The Normalized Difference Vegetation Index (NDVI) requires red and near-infrared bands and is widely used as an indicator of the chlorophyll content and density of a vegetated surface (Rouse et al., 1974). In this study PlanetScope satellite data were used. PlanetScope provides near-daily global imaging at optical wavelengths, observing in RGB and near-infrared at 3–5 m spatial resolution. This study used the Planet Fusion surface reflectance product, which represents a comprehensive harmonization and fusion methodology based on the CubeSat Enabled Spatio-Temporal Enhancement Method (CESTEM) (Planet, 2022; Houborg and McCabe, 2018b,a). Planet Fusion leverages rigorously calibrated publicly accessible datasets from Sentinel-2, Landsat 8/9, Moderate Resolution Imaging Spectroradiometer (MODIS), and Visible Infrared Imaging Radiometer Suite (VIIRS) in concert with the higher spatial and temporal resolution data provided by Planet's medium resolution constellation of 200+ CubeSats for full fleet interoperability. Planet Fusion includes rigorous, temporally driven, cloud and cloud shadow detection and advanced harmonization to reduce cross-sensor inconsistencies resulting from variations in orbital configurations, spectral responses, and geometric and radiometric quality. The end result is a next generation analysis ready surface reflectance product that can be used to derive daily, cloud-free, and gap-free NDVI time series data characterized by enhanced radiometric stability and consistency across space and time to support studies on high-frequency vegetation dynamics (Planet, 2022; Aragon et al., 2021; Houborg and McCabe, 2018a). Finally, the observations were resampled at a 10 by 10 meter resolution to meet the spatial resolution of Sentinel-1 for a more accurate comparison.

3.2. Data analysis

3.2.1. Classifying fields by sucrose yield

First, the variation of vegetation indices per field were assessed over the growing season. To understand the response of the vegetation

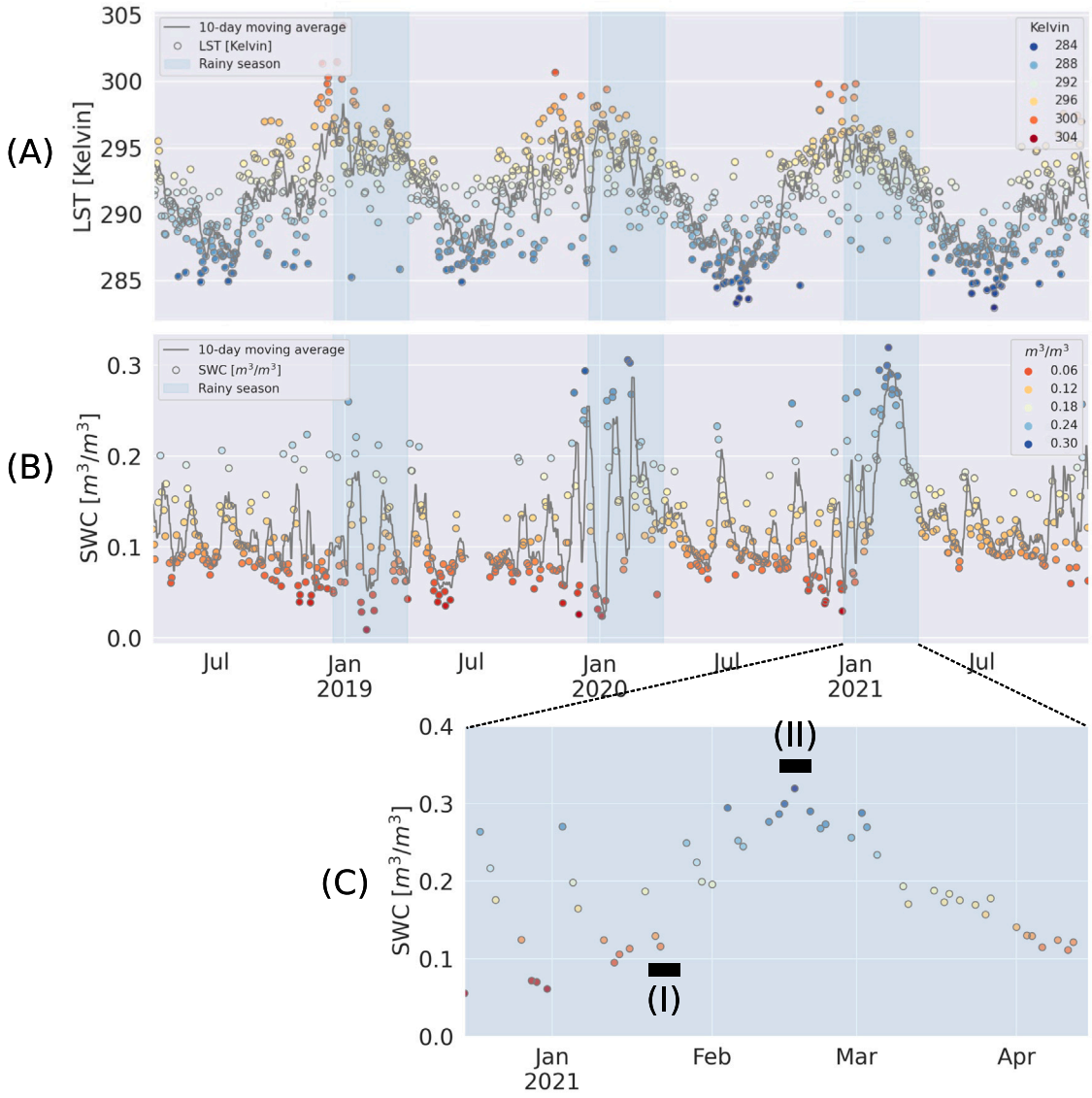

Fig. 4. (A) Land Surface Temperature and (B) soil water content averaged for all the fields under study from April 2018 until December 2021. The individual observations are indicated with colored dots. The gray line shows a moving average with a 10 day timeframe. The blue shading indicates the rainy season. (C) detailed view of the rainy season of 2021. (I) and (II) indicate before and during the waterlogging peak, respectively. (For interpretation of the references to color in this figure legend, the reader is referred to the web version of this article.)

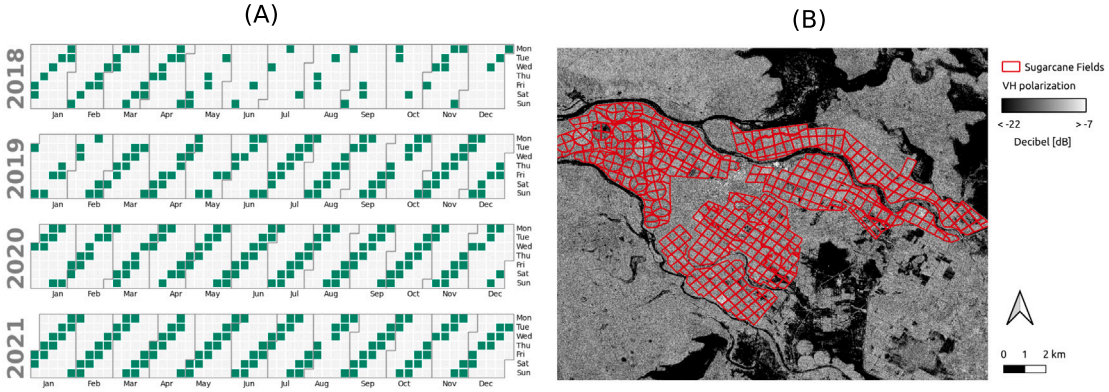

Fig. 5. (A) Green squares are days of Sentinel-1 observations used in the analysis (Tomkwok, 2022). (B) Snapshot of Sentinel-1 observation (2021-02-17) with fields under study in Xinavane, Mozambique. (For interpretation of the references to color in this figure legend, the reader is referred to the web version of this article.)

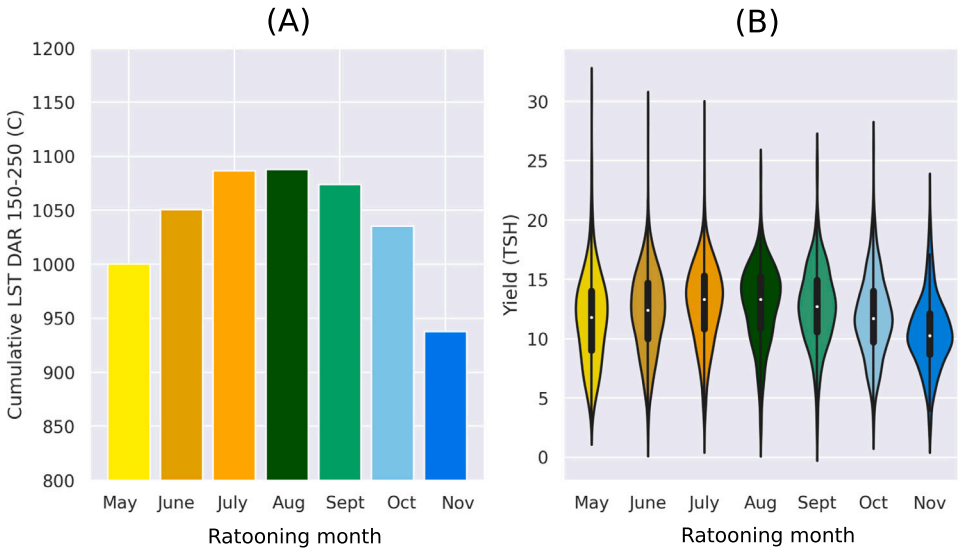

Fig. 6. (A) cumulative Land Surface Temperature between DAR 150–200 for fields with similar ratooning months (B) violin plot for average sucrose yield per ratooning month for season 2019, 2020, and 2021.

indices to sugarcane yield variability, the 25th, 50th, and 75th percentiles of the sucrose yield (TSH) dataset were calculated. From these percentiles four groups were created, respectively < 25th, 25th–50th, 50th–75th, > 75th. These yield constraints were used to mask the field time series and generate averages for different performance groups and different indices. A rolling mean of fifteen days was used to visualize time series.

3.2.2. Seasonality in sucrose development

Previous studies have found a connection between ratooning month, sugarcane biomass accumulation and sucrose yield (van Heerden et al., 2010). Due to seasonal variations in radiation, the relationship between biomass and intercepted radiation is affected by ratooning month. This means that radiation use efficiency for sugarcane varies depending on the ratooning month (Donaldson et al., 2008). Fig. 4 A shows how Land Surface Temperature (LST) varies during the year and Fig. 6 shows that yield is indeed affected by choice of ratooning month. Fig. 6 shows the difference in yield in the plantation can potentially be as much as 3 TSH [=20 percent] comparing the average yield in August and November.

Fig. 6 illustrates how the LST in the period of Day After Ratooning (DAR) 150–200 relates to the seasonality in yield. This implies, in order to compare other influential factor besides temperature, ratooning dates or month need to be considered. Therefore, the data were further sorted by ratooning month which ranges from May to November. April and December were excluded from the analysis due to insignificant number of fields harvested during these months. The categorization aimed to understand the effect of ratooning month on crop growth and how the vegetation indices are affected by other factors (e.g. large rainfall events).

3.2.3. Inter-annual variability

To demonstrate the difference between seasons, the average of the different observations for a specific Day of Ratooning was created for different growing seasons. Three seasons were used to compute these averages, season 2018–19, season 2019–2020, and season 2020–2021. In addition to time series, Pearson correlations between sucrose yield and polarizations, CR, and NDVI were also provided. The average value of these polarizations and indices in the last 150 days before the ratooning date were related to sucrose yield to understand the relationship to yield in different seasons.

3.2.4. The influence of waterlogging on sucrose monitoring

In this section we visualized mean backscatter over the time series of the VV, VH, and CR for fields ratooned in a given month. To illustrate the effect of waterlogging on backscatter we focused on the wet period in season 2020–2021 (see Fig. 4 (C)). The agricultural department in Xinavane confirmed that intense rainfall events combined with high groundwater levels due to the rise of water levels in the Incomati river, resulted in prolonged waterlogging during this period. To start with, the SWC and backscatter were compared in a season with a relatively dry rainy season (2018–19) and a relatively wet rainy season (2020–21) for similar ratooning months. Second, we compared data from at the waterlogging peak [2021-02-11:2021-02-18], to data from the local minimum before the waterlogging peak [2021-01-12:2021-01-19]. Each period contained three radar observations, which were averaged before visualizing the difference as a function of growth stage.

4. Results and discussion

4.1. Observing different sucrose levels

Figs. 7 shows the behavior of VH and VV backscatter and the CR during three different growing seasons. Figs. 7 (A), (D), and (G) show that the increase in biomass leads to an increase of around 5 dB in VH backscatter. Similar to the results of Molijn et al. (2019), there is a rapid increase at the start of the season and a slower decrease after the maximum is reached. However, the results are similar among the yield performance categories, particularly early in the season.

In contrast, results from the VV polarization in Fig. 7, (B), (E), and (H), are markedly different for the four yield performance classes. By the end of the season, the difference between the lowest and highest performing categories is 1.5 dB in VV compared to 0.5 dB in VH. The maxima are more distinct in VV compared to VH, and the rate of decrease after the maximum is also different. One reason for the clear distinction among yield categories in VV may be the predominantly vertical structure due to the sugarcane stalks. In addition, the stalk is the main reservoir of sucrose in the sugarcane crop (Wang et al., 2013) and sucrose yield data is directly linked and measured from the fresh stalk biomass, Section 2. Stalk biomass is lower in lower performing fields and higher in higher performing fields (Inman-Bamber et al., 2009).

The combined influence of the differences between VH and VV is encapsulated in the CR. Fig. 7 (C), (F), (I), shows a clear distinction

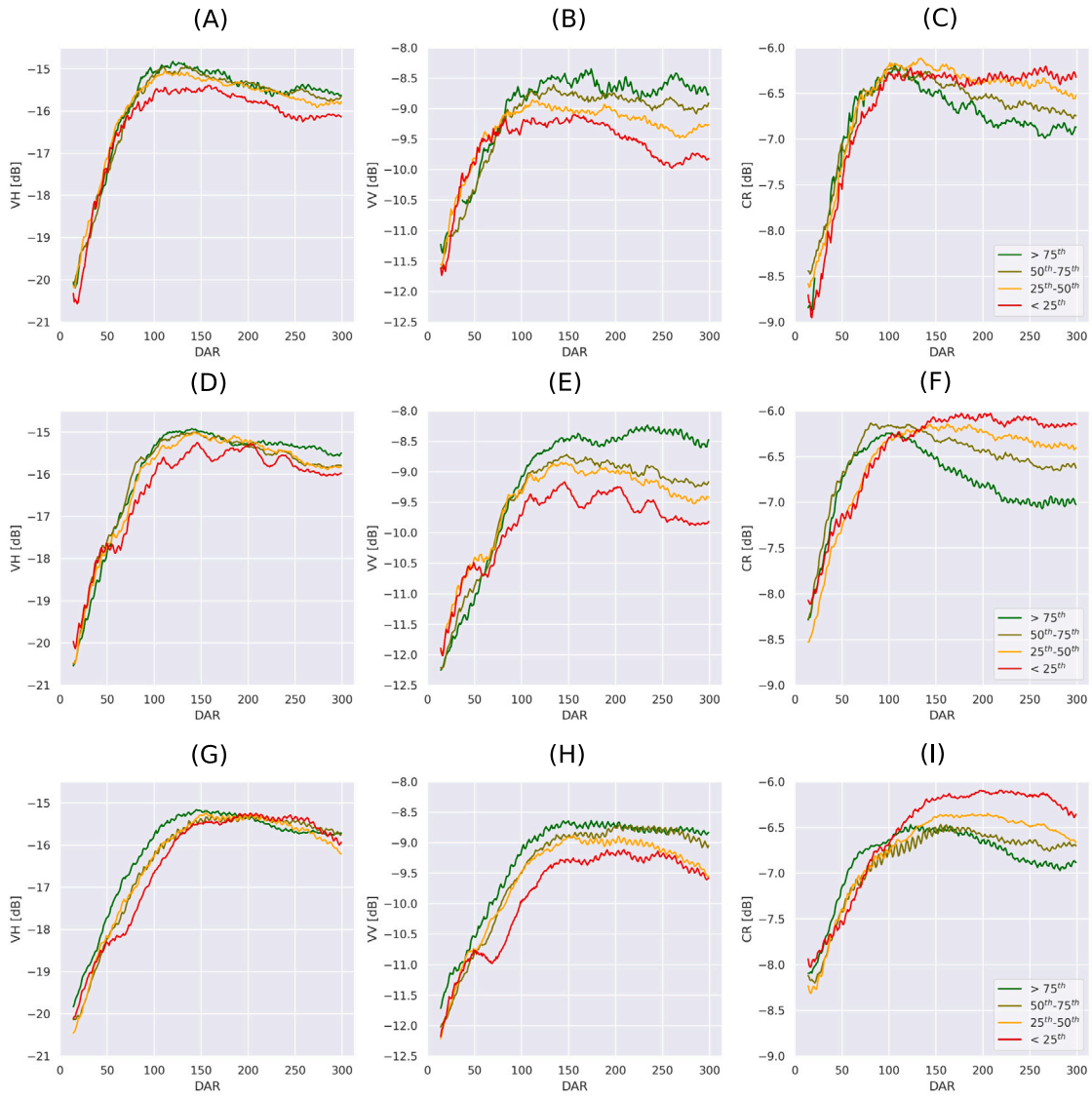

Fig. 7. The figures in the first columns (A), (D), and (G) show the development of VH over the growing season. Subsequently, the figures in the second column (B, E, and H) represent the VV and third column (C, F, and I) represent the CR. Each row represents a different season: 2018–2019, 2019–2020, and 2020–2021 (Day after Ratooning) respectively. The different colors represent the different sucrose yield percentiles over the growing season.

among the yield categories in the CR. The CR of lower yield categories increases more slowly, and reaches a maximum 50 to 75 days later than the higher yield categories. The maximum values themselves are higher for the lower yield categories. The most notable feature, though, is the divergence after the maximum has been reached. The CR from the lowest yield category stays close to its maximum until harvest, while the CR of the highest yield category has the sharpest decline. By the end of the season, the difference in CR between the highest and lowest yield categories can be as high as 1 dB (Fig. 7 (F)). Furthermore, den Besten et al. (2021a) used published data and modeling to argue that sucrose accumulation decreases the dielectric constant of sugarcane, thereby lowering the Sentinel-1 backscatter. A decrease of the dielectric constant due to an increase in sucrose concentration was also observed by Sumranbumrung et al. (2021). This explains why higher performance categories show lower CR values over the growing season, and vice versa. Fig. 7 (C), (F), (I) confirms the CR is indicative of the measured VWC, as pointed out by other studies (Veloso et al., 2017; Vreugdenhil et al., 2018).

Recall that the vertical distribution of moisture and sucrose is not uniform, and is different for higher and lower yielding sugarcane (Fig. 1) (Inman-Bamber et al., 2009). In higher yielding sugarcane, the ratio of moisture to sucrose is more vertically homogeneous, while there is a gradient in lower yielding stalks. However, even in higher yielding sugarcane, there is little to no sucrose at the top of the plant. Note though, that the dynamics of total backscatter are not necessarily dominated by the top of the canopy, or some sensing depth from the top of the canopy. Recent modeling at L-band has also shown that contributions to total backscatter depend on the vertical distribution of moisture, or more generally on the vertical variations in dielectric constant (Vermunt et al., 2022). InSAR studies have also shown that the phase center can be close to the surface even for relatively high frequencies (Joerg et al., 2018; Steele-Dunne et al., 2017). This explains why, even at C-band, Sentinel-1 backscatter is sensitive to dynamics in sucrose accumulation within the stalk and allows for a distinction between sugarcane with high and low sucrose yield.

In Fig. 8 the development of VH, VV, CR, and NDVI over all three growing seasons are visualized. Fig. 8 (D) and (E) shows CR and NDVI are able to distinguish different performance groups over the growing season. In particular, the lowest performance category deviates early in the season from the other categories. This may suggest poor performing fields are more easily detectable early in the season. The maximum of the VH, VV and CR radar data is observed earlier than the maximum

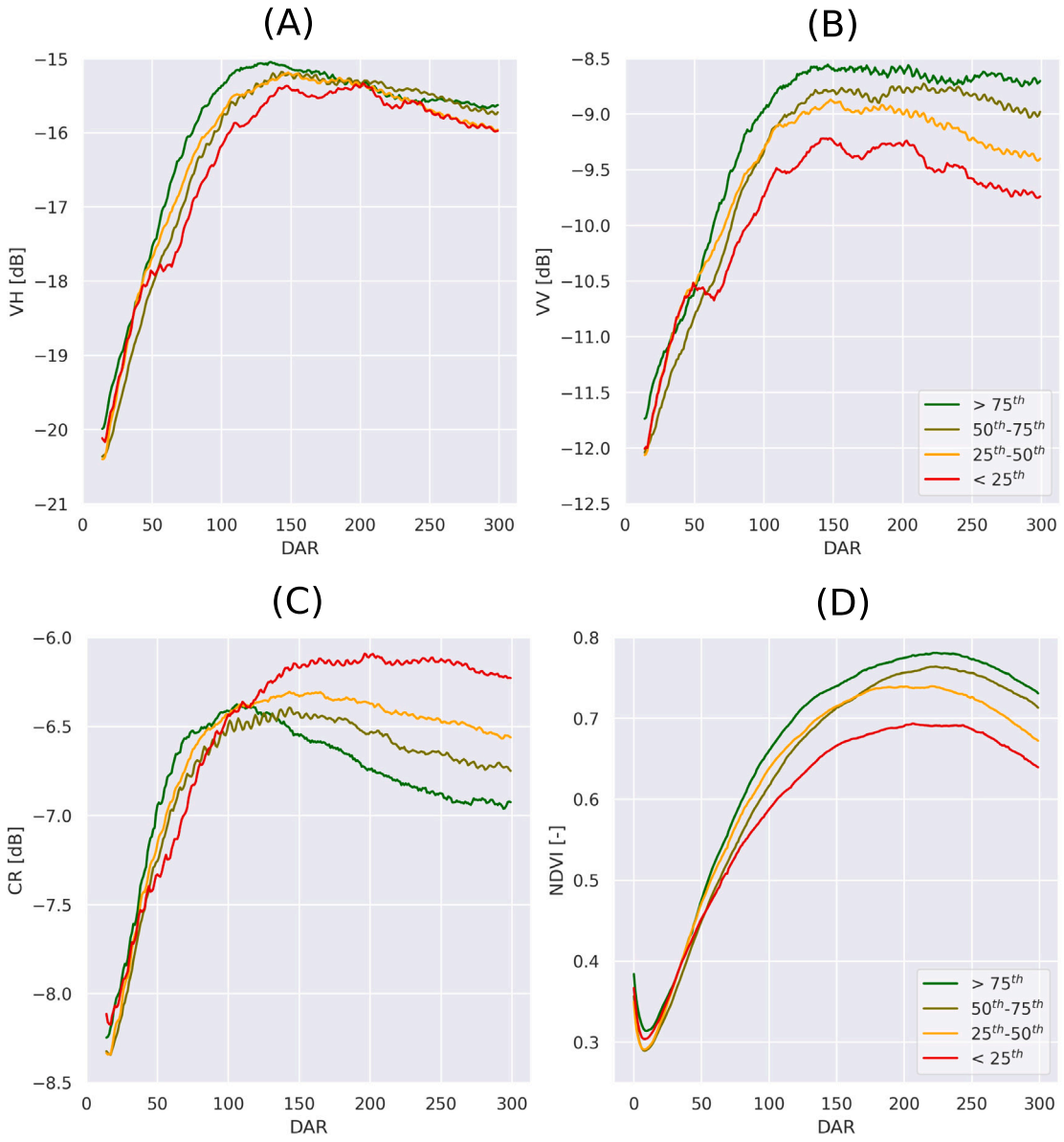

Fig. 8. The development of (A) VH, (B) VV, (C) CR, and (D) NDVI over the growing season combining all seasons (Day after Ratooning). The different colors represent the different sucrose yield percentiles over the growing season.

in the optical indices. This was also observed by Molijn et al. (2019). More importantly, while the lowest category deviates from the others in the optical indices early in the season, the distinction between all four classes is clearer in the radar data. In particular there is a delay between the classes during the development stage. In addition, Table 1 shows the correlation between backscatter and sucrose yield in the different seasons. The VV polarization and sucrose yield show moderate positive correlations in Season 2018–19 and Season 2019–20.

4.2. Seasonality in sucrose development

Fig. 9 (A), (B), and (C) shows the influence of ratooning month on the evolution of backscatter. The influence of the choice of ratooning month on crop yield is visible in VV, VH, and CR. In VV, VH and CR the fields ratooned in October and November rise to their maximum faster than other months. However, in the VV and VH data these fields end up distinctly lower at the end of the growing season. This is very consistent with Fig. 6 (B), which shows that fields ratooned in the months October and November have a lower yield compared to other ratooning months.

Compared to NDVI in Fig. 9 (D), the development is similar to the individual polarizations. Fields ratooned in October or November, for instance, rise faster, but finish with the lowest average values. This illustrates the importance of temperature on sucrose development. Fields ratooned in October or November experience high temperatures at the start of the growing season.

In addition, Fig. 9 illustrates the difference in temporal behavior between optical and radar timeseries. Where NDVI shows a clear distinction between ratooning months, it is evident backscatter records more than vegetation. For example, in Fig. 9 (C) the CR for ratooning month November shows a steep rise due to high initial temperatures and reaching a maximum at DAR 75. After reaching this maximum a second high is reached at DAR 100, coinciding with the onset of the rainy season, which commences at the end of December or January (see Section 3.2). This is also visible in the ratooning month of August in the CR, a second peak is reached around DAR 200 in Fig. 9 (C), which coincides with the onset of the rainy season. These additional peaks are not visible in NDVI in Fig. 9 (D). It is known that backscatter is sensitive to soil moisture and the soil surface in early growth stages (de Roo

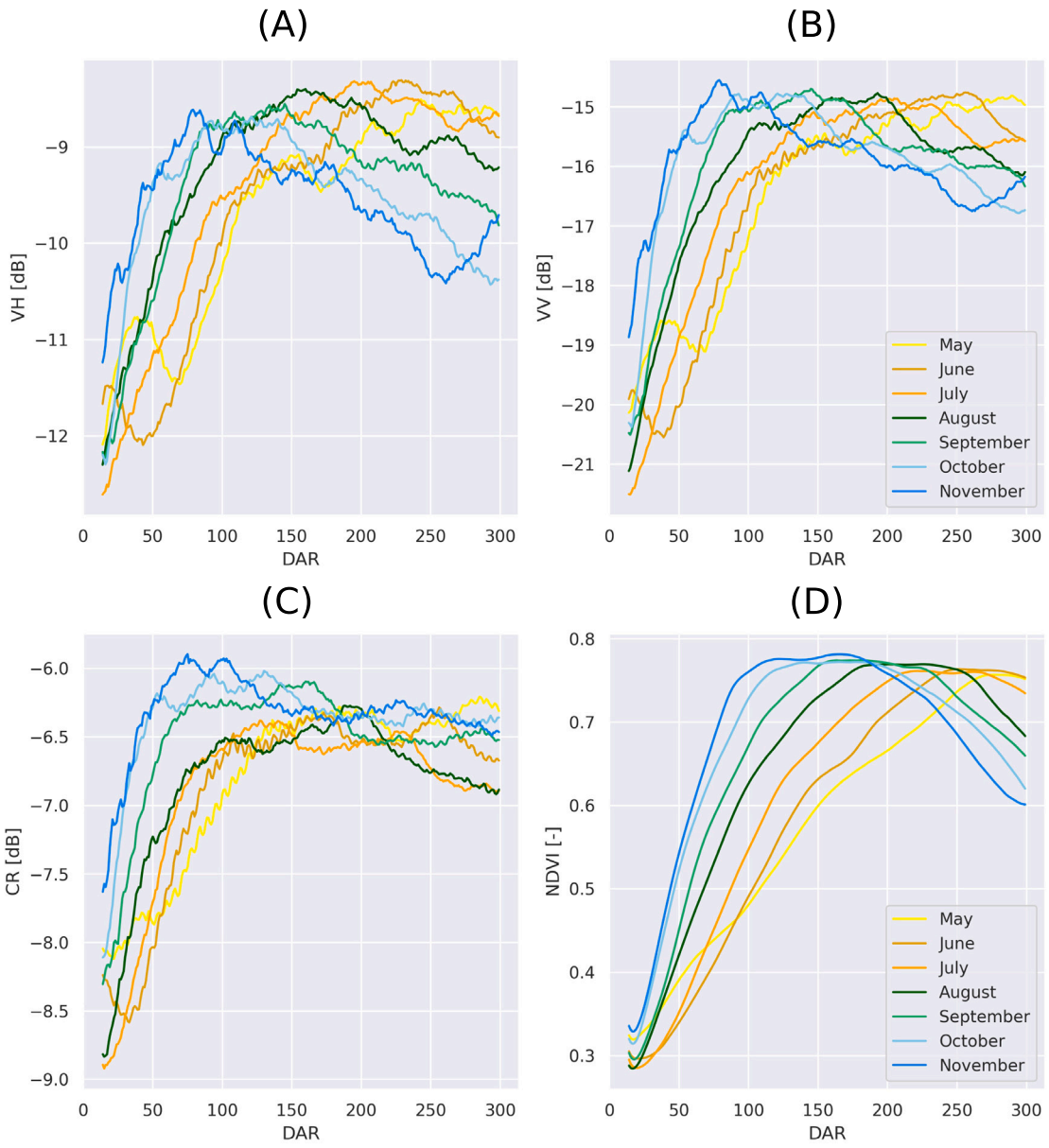

Fig. 9. The average (A) VH, (B) VV, (C) CR, and (D) NDVI over the growing season (Day After Ratooning) for different ratooning months. The colors indicate the different ratooning months.

Table 1
This table shows the Pearson correlation between mean backscatter in the last 150 days of the growing season observed in different polarizations, the CR, NDVI, and sucrose yield (TSH) for seasons 2018–19, 2019–20, 2020–21 and all three seasons together.

	Season 2018–19	Season 2019–20	Season 2020–21	All seasons
VV	0.55	0.52	0.22	0.53
VH	0.22	0.21	−0.11	0.19
CR	−0.48	−0.54	−0.49	−0.56
NDVI	0.58	0.6	0.34	0.6

et al., 2001; Pierdicca et al., 2017). However, it may be worthwhile to also consider the effect of extreme wet periods throughout the growing season.

4.3. Inter-year variability

Table 1 shows generally higher correlations between NDVI and sucrose yield than backscatter observations and sucrose yield in different seasons. For backscatter, the CR and VV give highest correlations to the yield. The correlation with CR is variable ranging from −0.48 - −0.56, whereas the correlation between VV and sucrose yield lay between 0.22 and 0.55. Interestingly, all correlations except CR are affected in season 2020–21. The VH backscatter and sucrose yield in season 2020–21 is even negative opposing the correlation in other seasons.

Fig. 10 shows the mean over the growing season for VV, VH, CR, and NDVI as a function of day after ratooning. In Fig. 10 (C) and (D) it is clearly visible season 2020–21 is behaving differently than other seasons. The graphs show a delay in the sugarcane development. Fig. 11 (A), (C), and (D) show the standard deviation is also different in season 2020–21. In this season a long wet period was documented, resulting into prolonged waterlogging, see Section 3.2.4.

4.4. The influence of waterlogging on sugarcane monitoring

Fig. 12 shows (A) the average Soil Water Content and (B) average VH polarization for fields with a ratooning month in June in two different seasons, season 2018–2019 (red) and season 2020–2021 (blue).

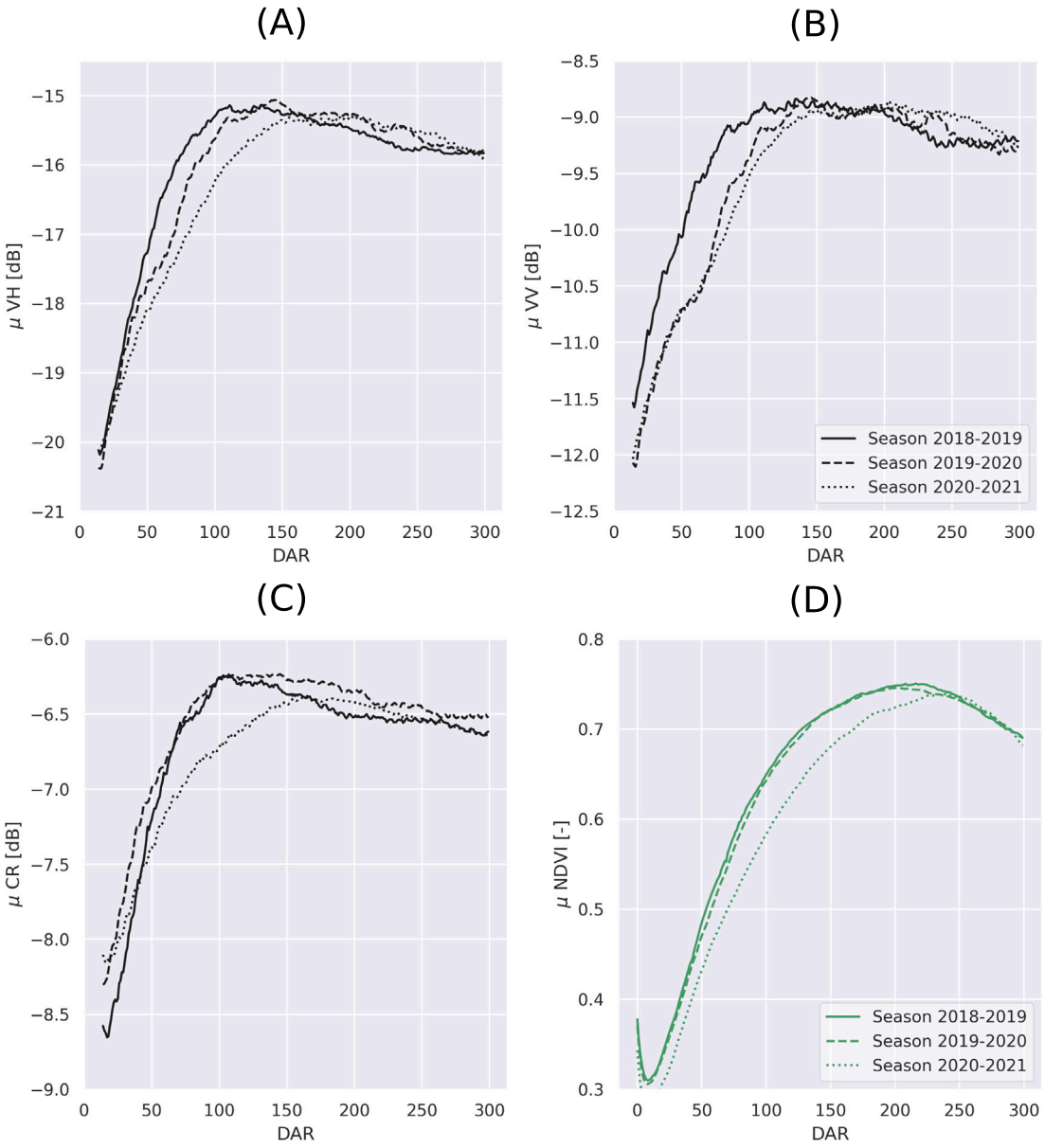

Fig. 10. The average (A) VH, (B) VV, (C) CR, and (D) NDVI over the growing season for seasons 2018–2019, 2019–2020, and 2020–2021. (Day after Ratooning).

Fig. 12 illustrates the response of VH backscatter due to the rainy season. In both seasons an increased Soil Water Content in Fig. 12 (A) in mid-February and a drydown towards April is visible in VH backscatter in Fig. 12 (B). The rainy season was less intense in season 2018–2019 than in 2020–2021, which resulted in a long waterlogging event in 2021. Considering the waterlogging event, as identified in Section 3.2.4, the blue shaded area (II) identifies the peak of the waterlogging event in 2021 and (I) before the waterlogging event. The difference between VH backscatter at the height of the peak (II) and before the rise of the peak (I) is also visible in Fig. 12 (B) in season 2020–2021. Similar figures for different ratooning months can be found in the appendix.

To further quantify the effect of the waterlogging event on backscatter, Fig. 13 shows the difference in the period before the large soil water content peak in season 2020–21 and during the peak for different ratooning months. The difference shows backscatter increases as a result of the event and is visible in VH, VV and CR. The waterlogging event causes differences between 0.45 dB and 1 dB for VV, and between 1.12 to 1.47 dB for VH. The higher values in November in the individual polarizations indicate that the effect of waterlogging is more visible at earlier stages of the crop growth, i.e. when the canopy is not fully developed yet. The results of CR in Fig. 13 also indicate that the effect of waterlogging may be translated through to the cross ratio. Therefore, the CR contains information on waterlogging.

Though few studies have explicitly considered waterlogging, these differences can be considered in the context of what is known about flooding under vegetation more generally. Lang et al. (2008) researched the difference of flooded and non-flooded forest in HH polarization (C-band) and recorded an average difference of 2.45 db depending on the incidence angle. Sentinel-1 data was also used to detect temporary flooded vegetation (TFV) to improve flood algorithms (Tsyganskaya et al., 2018). Tsyganskaya et al. (2018) found, in different parts of the world, that VH and VV increased during flooding events and the increase was due to the interaction between standing water and the vertically oriented vegetation which increases the double- or multi-bounce interactions (Tsyganskaya et al., 2018).

Despite sugarcane's thick canopy, Fig. 13 shows that waterlogging is visible in all crop stages. It seems that the effect of waterlogging is

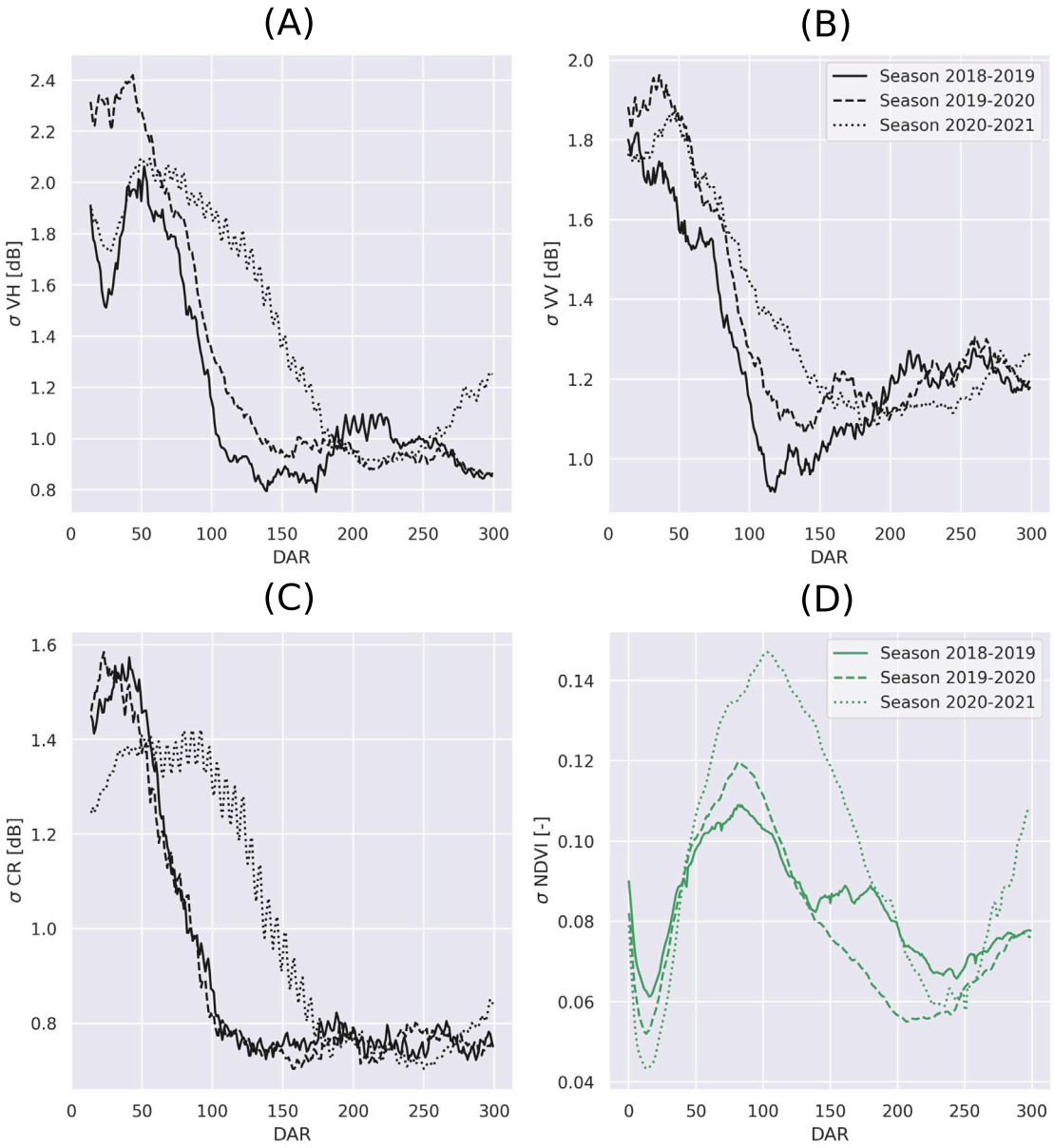

Fig. 11. The standard deviation VH, VV, CR, and NDVI over the growing season for seasons 2018–2019, 2019–2020, and 2020–2021. (Day after Ratooning).

more evident at earlier stages of the growing season (ratooning month November) in the individual polarizations. The results imply Sentinel-1 backscatter contains both information on waterlogging under the canopy as well as sucrose development in the stalk. Therefore, CR could potentially play a role in the discrimination of waterlogging.

5. Conclusion

The aim of this research was to understand how Sentinel-1 backscatter responds to sugarcane yield variability and waterlogging. We demonstrated the possibility to monitor sugarcane yield throughout the season, the effect of ratooning month on sugarcane development, and how waterlogging under the canopy is observed within different stages during the sugarcane development. All this valuable information is evidently present in Sentinel-1 backscatter.

The results showed VV backscatter contains information on sucrose development. The VV backscatter responds to the stalk characteristics which is also the reservoir of sucrose in the sugarcane crop. The CR represents the VWC in the stalk and the results demonstrated the influence of the distribution in availability of moisture and sucrose in the stalk on total observed backscatter. The fraction of sucrose and VWC changes over the growing season and the vertical distribution of sucrose and VWC varies as well. The results showed both influence the observed backscatter.

In addition, the results demonstrated the influence of choice in ratooning month on the sucrose yield and consequently backscatter. By considering ratooning month and comparing sucrose yield with different backscatter observations, we discovered the influence of waterlogging beneath the sugarcane canopy. Especially the VH backscatter was found to be sensitive to waterlogging beneath a canopy. However, waterlogging was also visible in the CR, which demonstrates the CR can be used to discriminate waterlogging from regular crop growth conditions. Moreover, the analysis implies the influence of waterlogging is present in all stages of the sugarcane growth, despite a thick sugarcane canopy.

The results of this research indicate that Sentinel-1 backscatter contains both information on waterlogging under the canopy as well as sucrose development in the plant. As the influence of waterlogging is detectable on a field-scale, it gives confidence that Sentinel-1

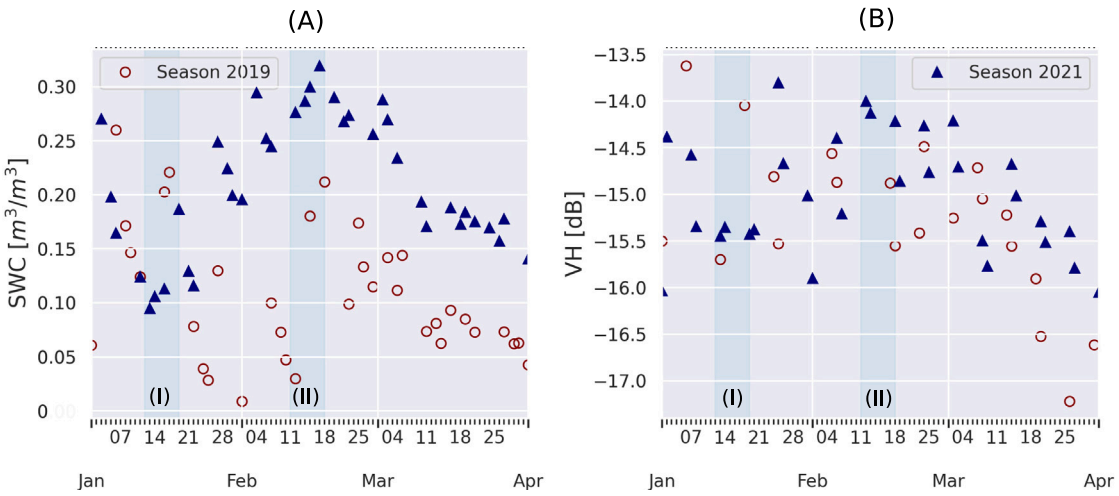

Fig. 12. The average Soil Water Content (A) and average VH backscatter (B) for fields ratooned in August for Season 2018–2019 and 2019–2020. The graphs zoom in on the period of the 1st of January until the 1st of April. (I) and (II) indicate the period before and during the waterlogging event in Season 2020–2021. (For interpretation of the references to color in this figure legend, the reader is referred to the web version of this article.)

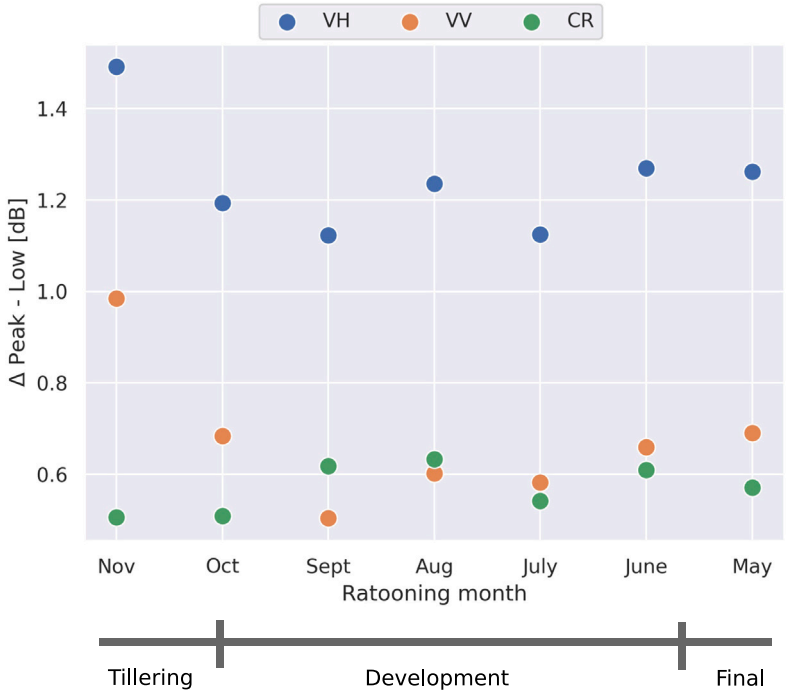

Fig. 13. The difference between backscatter during and before the waterlogging peak averaged for fields with similar ratooning months.

backscatter can be used to monitor waterlogging. Also, the influence of waterlogging can be flagged to help interpret vegetation signals retrieved with Sentinel-1 backscatter.

We recommend future studies and applications on crop monitoring with backscatter to consider waterlogging or inundation within the growing season. In addition, more experimental research is needed to understand the vertical and temporal distribution of sucrose and moisture and its effect on backscatter for different crops. This is necessary to improve understanding of the actual sensing depth of backscatter and to understand the contributions of different surface and crop characteristics on backscatter retrievals. Here, modeling studies could contribute to increased understanding of the backscatter signal.

Sentinel-1 backscatter contains a lot of information relevant to monitor sugarcane development. Nevertheless, more collaboration is needed between radar remote sensing experts and application users to extract relevant and actionable information about the surface and canopy. In addition, such collaboration would allow remote sensing scientists to benefit from the great wealth of data collected on the ground by agriculturalists every season.

CRediT authorship contribution statement

Nadja den Besten: Conceptualization, Formal analysis, Data curation, Writing – original draft. **Susan Steele Dunne:** Conceptualization, Writing – original draft. **Ashfak Mahmud:** Data curation, Visualization. **Daniel Jackson:** Visualization, Writing – review & editing. **Benjamin Aouizerats:** Writing – review & editing. **Richard de Jeu:** Conceptualization. **Rogier Burger:** Data curation. **Rasmus Houborg:** Data curation, Writing – review & editing. **Mark McGlinchey:** Writing – review & editing. **Pieter van der Zaag:** Supervision.

Declaration of competing interest

The authors declare that they have no known competing financial interests or personal relationships that could have appeared to influence the work reported in this paper.

Data availability

Data will be made available on request.

Appendix A. Supplementary data

Supplementary material related to this article can be found online at https://doi.org/10.1016/j.rse.2023.113555.

References

Aragon, B., Ziliani, M.G., Houborg, R., Franz, T.E., McCabe, M.F., 2021. CubeSats deliver new insights into agricultural water use at daily and 3 m resolutions. Sci. Rep. 11 (1), 1–12.

Baghdadi, N., Boyer, N., Todoroff, P., El Hajj, M., Bégué, A., 2009. Potential of SAR sensors terrasar-X, ASAR/ENVISAT and PALSAR/ALOS for monitoring sugarcane crops on reunion island. Remote Sens. Environ. 113 (8), 1724–1738.

Bégué, A., Arvor, D., Bellon, B., Betbeder, J., De Abelleyra, D., Ferraz, R.P.D., Lebourgeois, V., Lelong, C., Simões, M., Verón, S.R., 2018. Remote sensing and cropping practices: A review. Remote Sens. 10 (1), http://dx.doi.org/10.3390/rs10010099, URL https://www.mdpi.com/2072-4292/10/1/99.

Bégué, A., Lebourgeois, V., Bappel, E., Todoroff, P., Pellegrino, A., Baillarin, F., Siegmund, B., 2010. Spatio-temporal variability of sugarcane fields and recommendations for yield forecast using NDVI. Int. J. Remote Sens. 31 (20), 5391–5407.

Bocca, F.F., Rodrigues, L.H.A., Arraes, N.A.M., 2015. When do I want to know and why? Different demands on sugarcane yield predictions. Agricult. Sys. 135, 48–56.

Bordonal, R.d.O., Carvalho, J.L.N., Lal, R., de Figueiredo, E.B., de Oliveira, B.G., La Scala, N., 2018. Sustainability of sugarcane production in Brazil. a review. Agron. Sustain. Dev. 38 (2), 1–23.

Butler, D., 2001. The performance of sugarcane varieties N23 and N25 on low yield potential soils in swaziland. In: Proc S Afr Sug Technol Ass. 75, pp. 165–170.

Cancela, J.J., González, X.P., Vilanova, M., Mirás-Avalos, J.M., 2019. Water management using drones and satellites in agriculture. Water 11 (5), URL https://www.mdpi.com/2073-4441/11/5/874.

Cock, J., 2001. Sugarcane growth and development. Sugarcane Int. 5–15.

de Jeu, R., De Nijs, A., Van Klink, M., 2016. Method and system for improving the resolution of sensor data.

de Roo, R.D., Du, Y., Ulaby, F.T., Dobson, M.C., 2001. A semi-empirical backscattering model at L-band and C-band for a soybean canopy with soil moisture inversion. IEEE Trans. Geosci. Remote Sens. 39 (4), 864–872.

den Besten, N., Kassing, R., Muchanga, E., Earnshaw, C., de Jeu, R., Karimi, P., van der Zaag, P., 2020. A novel approach to the use of earth observation to estimate daily evaporation in a sugarcane plantation in xinavane, mozambique. Phys. Chem. Earth A/B/C 102940.

den Besten, N., Steele-Dunne, S., Aouizerats, B., Zajdband, A., De Jeu, R., Van Der Zaag, P., 2021a. Observing sucrose accumulation with sentinel-1 backscatter. Front. Remote Sens. 2, 1–9.

den Besten, N., Steele-Dunne, S., de Jeu, R., van der Zaag, P., 2021b. Towards monitoring waterlogging with remote sensing for sustainable irrigated agriculture. Remote Sens. 13 (15), 2929.

Donaldson, R., Redshaw, K., Rhodes, R., Antwerpen, R.v., et al., 2008. Season effects on productivity of some commercial South African sugarcane cultivars, II: Trash production. In: Proceedings of the Annual Congress-South African Sugar Technologists' Association. (81), South African Sugar Technologists' Association, pp. 528–538.

Doorenbos, J., Kassam, A., 1979. Yield response to water. Irrigation Drain. Pap. 33, 257.

ESA, 2021. Sentinel-1 observation scenario. https://sentinels.copernicus.eu/web/sentinel/missions/sentinel-1/observation-scenario, (Accessed 7 July 2021).

FAO, 2016. Coping with water scarcity in agriculture a global framework for action in a changing climate. http://www.fao.org/3/a-i6459e.pdf.

Fernandes, J.L., Ebecken, N.F.F., Esquerdo, J.C.D.M., 2017. Sugarcane yield prediction in Brazil using NDVI time series and neural networks ensemble. Int. J. Remote Sens. 38 (16), 4631–4644.

Holmes, T., De Jeu, R., Owe, M., Dolman, A., 2009. Land surface temperature from ka band (37 GHz) passive microwave observations. J. Geophys. Res.: Atmos. 114 (D4).

Houborg, R., McCabe, M.F., 2018a. A cubesat enabled spatio-temporal enhancement method (cestem) utilizing planet, landsat and modis data. Remote Sens. Environ. 209, 211–226.

Houborg, R., McCabe, M.F., 2018b. Daily retrieval of NDVI and LAI at 3 m resolution via the fusion of CubeSat, landsat, and MODIS data. Remote Sens. 10 (6), 890.

Inman-Bamber, G., 2013. Sugarcane yields and yield-limiting processes. Sugarcane: Physiol. Biochem. Funct. Biol. 579–600.

Inman-Bamber, N., Bonnett, G., Spillman, M., Hewitt, M., Xu, J., 2009. Source–sink differences in genotypes and water regimes influencing sucrose accumulation in sugarcane stalks. Crop Pasture Sci. 60 (4), 316–327.

Joerg, H., Pardini, M., Hajnsek, I., Papathanassiou, K.P., 2018. Sensitivity of SAR tomography to the phenological cycle of agricultural crops at X-, C-, and L-band. IEEE J. Sel. Top. Appl. Earth Obs. Remote Sens. 11 (9), 3014–3029.

Khabbazan, S., Vermunt, P., Steele-Dunne, S., Ratering Arntz, L., Marinetti, C., van der Valk, D., Iannini, L., Molijn, R., Westerdijk, K., van der Sande, C., 2019. Crop monitoring using sentinel-1 data: A case study from The Netherlands. Remote Sens. 11 (16), 1887.

Lang, M.W., Townsend, P.A., Kasischke, E.S., 2008. Influence of incidence angle on detecting flooded forests using C-HH synthetic aperture radar data. Remote Sens. Environ. 112 (10), 3898–3907.

Lofton, J., Tubana, B.S., Kanke, Y., Teboh, J., Viator, H., Dalen, M., 2012. Estimating sugarcane yield potential using an in-season determination of normalized difference vegetative index. Sensors 12 (6), 7529–7547.

Mancini, A., Frontoni, E., Zingaretti, P., 2019. Satellite and uav data for precision agriculture applications. In: 2019 International Conference on Unmanned Aircraft Systems. ICUAS, IEEE, pp. 491–497.

Martinez-Feria, R.A., Basso, B., 2020. Unstable crop yields reveal opportunities for site-specific adaptations to climate variability. Sci. Rep. 10 (1), 1–10.

McCabe, M.F., Houborg, R., Lucieer, A., 2016. High-resolution sensing for precision agriculture: from earth-observing satellites to unmanned aerial vehicles. In: Remote Sensing for Agriculture, Ecosystems, and Hydrology XVIII, Vol. 9998. SPIE, pp. 346–355.

McNairn, H., Brisco, B., 2004. The application of C-band polarimetric SAR for agriculture: A review. Can. J. Remote Sens. 30 (3), 525–542.

Molijn, R.A., Iannini, L., Vieira Rocha, J., Hanssen, R.F., 2019. Sugarcane productivity mapping through C-band and L-band SAR and optical satellite imagery. Remote Sens. 11 (9), 1109.

Morel, J., Todoroff, P., Bégué, A., Bury, A., Martiné, J.-F., Petit, M., 2014. Toward a satellite-based system of sugarcane yield estimation and forecasting in smallholder farming conditions: A case study on reunion island. Remote Sens. 6 (7), 6620–6635.

Muchow, R., Robertson, M., Wood, A., 1996. Growth of sugarcane under high input conditions in tropical Australia. II. Sucrose accumulation and commercial yield. Field Crops Res. 48 (1), 27–36.

Mustafa, G., Joyia, F.A., Anwar, S., Parvaiz, A., Khan, M.S., 2018. Biotechnological interventions for the improvement of sugarcane crop and sugar production. Sugarcane-Technol. Res. IntechOpen: London, UK 113–138.

Owe, M., de Jeu, R., Holmes, T., 2008. Multisensor historical climatology of satellite-derived global land surface moisture. J. Geophys. Res. Earth Surf. 113 (F1).

Pierdicca, N., Pulvirenti, L., Boni, G., Squicciarino, G., Chini, M., 2017. Mapping flooded vegetation using COSMO-SkyMed: comparison with polarimetric and optical data over rice fields. IEEE J. Sel. Top. Appl. Earth Obs. Remote Sens. 10 (6), 2650–2662.

Planet, 2022. Planet fusion monitoring - technical specification, Version 1.0.0 ed. San Francisco, CA, URLhttps://support.planet.com/hc/en-us/articles/4406292582673-Planet-Fusion-Monitoring-Technical-Specification.html.

Rouse, J.W., Haas, R.H., Schell, J.A., Deering, D.W., et al., 1974. Monitoring vegetation systems in the great plains with ERTS. NASA Special Publ. 351 (1974), 309.

Shabbir, R., Javed, T., Afzal, I., Sabagh, A.E., Ali, A., Vicente, O., Chen, P., 2021. Modern biotechnologies: Innovative and sustainable approaches for the improvement of sugarcane tolerance to environmental stresses. Agronomy 11 (6), 1042.

Shaw, R.E., Meyer, W.S., McNeill, A., Tyerman, S.D., 2013. Waterlogging in Australian agricultural landscapes: a review of plant responses and crop models. Crop Pasture Sci. 64 (6), 549–562.

Shendryk, Y., Davy, R., Thorburn, P., 2021. Integrating satellite imagery and environmental data to predict field-level cane and sugar yields in Australia using machine learning. Field Crops Res. 260, 107984.

Silva, V., Garcêz, S., Silva, B.d., Albuquerque, M.d., Almeida, R., 2015. Métodos de estimativa da evapotranspiração da cultura da cana-de-açúcar em condições de sequeiro. Revista Brasileira de Engenharia AgríCola E Ambiental 19 (5), 411–417.

Som-ard, J., Atzberger, C., Izquierdo-Verdiguier, E., Vuolo, F., Immitzer, M., 2021. Remote sensing applications in sugarcane cultivation: A review. Remote Sens. 13 (20), URL https://www.mdpi.com/2072-4292/13/20/4040.

Steele-Dunne, S.C., McNairn, H., Monsivais-Huertero, A., Judge, J., Liu, P.-W., Papathanassiou, K., 2017. Radar remote sensing of agricultural canopies: A review. IEEE J. Sel. Top. Appl. Earth Obs. Remote Sens. 10 (5), 2249–2273.

Sumranbumrung, R., Khunkitti, P., Siritaratiwat, A., Kruesubthaworn, A., 2021. Characterization model of dielectric properties of cane sugar solution over 0.5–14 GHz. IEEE Trans. Instrum. Meas. 70, 1–8.

Surendran, U., Ramesh, V., Jayakumar, M., Marimuthu, S., Sridevi, G., 2016. Improved sugarcane productivity with tillage and trash management practices in semi arid tropical agro ecosystem in India. Soil Tillage Res. 158, 10–21.

Tomkwok, 2022. Calendar heatmaps from pandas time series data. GitHub Repository, https://github.com/tomkwok/calplot.

Tsyganskaya, V., Martinis, S., Marzahn, P., Ludwig, R., 2018. Detection of temporary flooded vegetation using sentinel-1 time series data. Remote Sens. 10 (8), 1286.
Ulaby, F.T., Jedlicka, R., 1984. Microwave dielectric properties of plant materials. IEEE Trans. Geosci. Remote Sens. (4), 406–415.
van der Schalie, R., de Jeu, R.A., Kerr, Y., Wigneron, J.-P., Rodríguez-Fernández, N.J., Al-Yaari, A., Parinussa, R.M., Mecklenburg, S., Drusch, M., 2017. The merging of radiative transfer based surface soil moisture data from SMOS and AMSR-e. Remote Sens. Environ. 189, 180–193.
van Heerden, P.D., Donaldson, R.A., Watt, D.A., Singels, A., 2010. Biomass accumulation in sugarcane: unravelling the factors underpinning reduced growth phenomena. J. Exp. Bot. 61 (11), 2877–2887.
Veloso, A., Mermoz, S., Bouvet, A., Le Toan, T., Planells, M., Dejoux, J.-F., Ceschia, E., 2017. Understanding the temporal behavior of crops using sentinel-1 and sentinel-2-like data for agricultural applications. Remote Sens. Environ. 199, 415–426.
Vermunt, P.C., Steele-Dunne, S.C., Khabbazan, S., Kumar, V., Judge, J., 2022. Towards understanding the influence of vertical water distribution on radar backscatter from vegetation using a multi-layer water cloud model. Remote Sens. 14 (16), 3867.
Vreugdenhil, M., Wagner, W., Bauer-Marschallinger, B., Pfeil, I., Teubner, I., Rüdiger, C., Strauss, P., 2018. Sensitivity of sentinel-1 backscatter to vegetation dynamics: An Austrian case study. Remote Sens. 10 (9), 1396.
Wang, J., Nayak, S., Koch, K., Ming, R., 2013. Carbon partitioning in sugarcane (saccharum species). Front. Plant Sci. 4, 201.